31 March 1995

ELSEVIER

Chemical Physics Letters 235 (1995) 552–557

CHEMICAL PHYSICS LETTERS

Nonexponential relaxation in solid C_{60} via time-dependent singlet exciton annihilation

S.L. Dexheimer [a,b,1], W.A. Vareka [a,b], D. Mittleman [a,b], A. Zettl [a,b], C.V. Shank [a,b]

[a] *Materials Science Division, Lawrence Berkeley Laboratory, Berkeley, CA 94720, USA*
[b] *Department of Physics, University of California, Berkeley, CA 94720, USA*

Received 20 December 1994; in final form 14 January 1995

Abstract

We present measurements and detailed modeling of the dynamics of solid C_{60} following photoexcitation. Optical pulses 60 fs in duration centered at 620 nm are used to excite the lowest optical band, and the relaxation of the photoexcitations is measured using a time-resolved pump–probe technique. The response is shown quantitatively to follow a time-dependent singlet exciton annihilation process consistent with long-range Förster annihilation. This result is supported by measurements of the dependence of the relaxation on excitation density and probe wavelength, by comparison of the response in thin film, crystalline, and solution samples, and by numerical modeling.

C_{60} has attracted considerable interest as a potential new material for electronic and nonlinear optical applications. Studies of ultrafast optical dynamics in C_{60} have been carried out to investigate the time scale of the optical response and the mechanisms involved in the electronic dynamics. A number of time-resolved studies of fast dynamics in solid C_{60} have been reported [1–9], and have revealed complex nonexponential dynamics on femtosecond and longer time scales. This unusual nonexponential behavior has led to a great deal of speculation as to the physical origin of the relaxation processes, and a wide range of mechanisms have been proposed as contributing to the dynamics, including electronic relaxation processes such as carrier trapping processes characteristic of disordered semiconductors [1,9], free carrier scattering [4,8], intramolecular relaxation processes [6,7], excitonic interactions and annihilation [3–6], and lattice relaxation processes [2]. In this Letter, we present detailed measurements and modeling of the dynamics, and show that the nonexponential relaxation is dominated by singlet exciton annihilation, but in an unusual limiting case consistent with long-range Förster annihilation, which gives rise to non-Markovian behavior with an effective time-dependent annihilation rate. This conclusion is supported by measurements of the dependence of the relaxation on excitation density and probe wavelength, by comparison of the response in thin film, crystalline, and solution samples, and by numerical modeling, providing a quantitative understanding of the unusual dynamics in this new material.

In the solid state, C_{60} forms a molecular crystal in which the intermolecular interactions are weak rela-

[1] Present address: Los Alamos National Laboratory, MST-11, MS E548, Los Alamos, NM 87545, USA.

0009-2614/95/$09.50
SSDI 0009-2614(95)00171-9

tive to the covalent bonding within the individual C_{60} molecules, and the low-lying electronic states are well approximated by the molecular orbitals associated with individual molecules. The nature of these electronic states is reflected in the optical absorption spectrum, which consists of a series of broad bands corresponding to transitions between the molecular orbital-derived states [10]. The lowest energy feature in the absorption spectrum is derived from the transition between the h_u highest occupied molecular orbital (HOMO) and the t_{1u} lowest unoccupied molecular orbital (LUMO). This transition is symmetry forbidden, and owes its weak intensity to vibronic coupling.

In the work presented here, measurements of the dynamics in C_{60} following photoexcitation into the lowest optical band were made using a standard pump–probe technique. Optical pulses centered at 620 nm from a colliding-pulse mode-locked (CPM) dye laser were amplified in a copper vapor laser-pumped dye amplifier, resulting in pulses approximately 60 fs in duration at an 8 kHz repetition rate. This beam was split into separate pump, probe, and reference beams, and the change in sample transmittance induced by the pump pulse was measured as a function of pump–probe delay. Differential detection of the probe and reference beams in a pair of balanced photodiodes and lock-in amplification were used to improve the sensitivity. Additional measurements to investigate the wavelength dependence of the optical response were made using broadband probe pulses. These pulses were derived from the amplified CPM pulses by splitting off part of the beam and using standard pulse compression techniques [11] to produce pulses $\leqslant 10$ fs in duration containing wavelength components from 550 to 670 nm. Wavelength-resolved differential transmittance measurements were made using the relatively narrow-band 60 fs amplified CPM pulses as the pump and cross-polarized broadband compressed pulses as the probe, with wavelength resolution achieved by spectrally filtering the probe beam after it had passed through the sample.

C_{60} samples were prepared from C_{60} powder purified by column chromatography. Thin films having thicknesses ranging from ≈ 200 nm to 1 μm were prepared by thermal sublimation onto sapphire, quartz, or glass substrates. C_{60} crystals with a plate

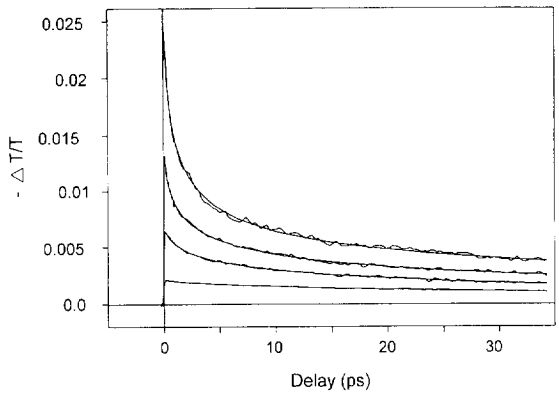

Fig. 1. Time-resolved negative differential transmittance at 620 nm of a C_{60} thin film following photoexcitation into the lowest optical band with pulses 60 fs in duration. Laser fluences (from top) are: 2.3, 1.3, 0.6, and 0.2 mJ/cm^2, corresponding to approximate excitation densities of 8.1×10^{19}, 4.4×10^{19}, 2.1×10^{19}, and 7.0×10^{18} cm^{-3}. The solid lines represent the results of fits to the time-dependent exciton annihilation process discussed in the text.

morphology were prepared by vapor transport. Saturated solutions of C_{60} were prepared in a mixture of benzene and toluene. To minimize the possibility of damage, the samples were maintained under an Ar atmosphere and were stored in the dark.

Fig. 1 shows traces of the time-resolved differential transmittance at 620 nm for a C_{60} thin film over a range of laser fluence values. The signals are presented as a negative differential transmittance $(-\Delta T/T)$, corresponding to an induced absorption as a result of photoexcitation. As previously noted [1–9], the time-dependent decay of the induced absorption is clearly nonexponential, and the signals show a strong dependence on excitation density, as will be discussed in detail below. For the data presented in Fig. 1, the pump and probe beams are orthogonally polarized so that scattered pump light that would otherwise contribute a dc offset to the signal can be rejected by a polarizer, and it is clear from the absence of signal at negative pump–probe delay times that the sample fully recovers to within the noise level between laser shots at the 8 kHz repetition rate of the laser system, thereby avoiding artifacts due to incomplete ground state recovery. Measurements with parallel pump and probe polarizations yield the same decay dynamics and signal amplitudes, aside from differences in the response within the duration of the pump pulse. Wavelength-

resolved measurements show no significant dependence of the nonexponential decay dynamics on probe wavelength throughout the range of 550 to 670 nm.

The observation of an induced absorption has been understood in terms of the energy level structure of C_{60}. The pump pulse excites the weak symmetry-forbidden HOMO–LUMO transition, populating LUMO states that present a substantially higher absorption cross section for the probe pulse than the HOMO states, owing to the presence of energetically accessible higher-lying electronic states to which transitions are symmetry allowed. An additional contribution may result from depopulation of the HOMO states by the pump pulse, which could allow transitions from lower-lying states into the empty HOMO states [4,7]. We note that the triplet state, which can be formed by intersystem crossing, has negligible absorption around 620 nm [12]. The decay of the observed induced absorption signal reflects the relaxation of the excited LUMO-derived singlet electronic states. The absence of a significant dependence of the decay dynamics on probe wavelength argues against energy relaxation within the excited electronic state as a dominant contribution to the nonexponential behavior and suggests that the same relaxation processes occur throughout the photoexcited optical band.

The most striking aspect of the nonexponential decay dynamics shown in Fig. 1 is the strong dependence of the shape of the decay curves on the excitation density. At the highest laser fluence value, the initial decay is very rapid, and this initial decay becomes progressively slower for lower laser fluence values. Since the data in Fig. 1 are presented as absolute signal levels (percentage change in transmission), another unusual aspect of the dynamics, its non-Markovian character, becomes apparent. In the small signal limit, the magnitude of the differential absorbance is simply proportional to the excited state population density, and for most decay processes, the slope of a decay curve at a given delay time is simply a function of the population density at that time. However, for the C_{60} data presented in Fig. 1, if for example, the initial slope of a low fluence decay curve is compared to the slope at a point corresponding to the same signal level, but farther out in time on a higher fluence decay curve, it is clear that the slopes of the curves are unequal. This shows that the dynamics are not simply a function of the total excited state population density, but rather that they depend on the history following excitation. Any successful model for the dynamics in solid C_{60} must reflect this non-Markovian behavior.

The strong dependence of the relaxation dynamics on excitation density is indicative of interactions between photoexcitations. An excitation density-dependent process that is well established in molecular crystals is exciton–exciton annihilation, or exciton fusion. In this case, the term exciton refers to a Frenkel-type exciton, as is expected to occur in solid C_{60}. Exciton annihilation is a nonradiative process involving the interaction of two excitations that results in a net depopulation of the excited state. The simple model usually applied to this two-body process is given by the second-order rate equation $dn/dt = -\gamma_0 n^2 - \beta n$, in which the annihilation rate is given by a constant, γ_0, and a term linear in population density is included to allow for an additional unimolecular decay process. This model assumes that the excitations diffuse sufficiently rapidly to maintain a spatially homogeneous excitation density, which allows the annihilation term to be written simply as $\gamma_0 n^2$. This model has been successfully applied to a wide range of studies in molecular crystals; however, it is clear that this simple equation cannot account for the non-Markovian behavior observed in C_{60}, since it gives a slope for the decay curve that is a function only of the population density.

Alternatively, in the limiting case that the excitations that remain spatially fixed, exciton annihilation via a Förster long-range resonance interaction [13,14] gives rise to an effective time-dependent annihilation rate reflected in the rate equation

$$dn/dt = -\gamma t^{-1/2} n^2 - \beta n. \tag{1}$$

The smooth lines in Fig. 1 represent fits to the solution to this rate equation,

$$n(t) = n(0)\exp(-\beta t) \times \left\{1 + \left(\pi^{1/2}\gamma n(0)/\beta^{1/2}\right) \times \mathrm{erf}\left[(\beta t)^{1/2}\right]\right\}^{-1}, \tag{2}$$

showing that this model successfully fits the dynamics in solid C_{60} over a wide range of excitation

densities. The data traces in Fig. 1 were fit over a time range excluding the duration of the pump pulse, giving a value $\gamma = (7 \pm 1) \times 10^{-15}$ cm^3 s$^{-1/2}$ for the annihilation constant and $\beta \approx 10^{10}$ s^{-1} for the linear decay term. In addition to the data presented in Fig. 1, decay traces were measured over a time range extending to 150 ps at low laser fluence values ($\leqslant 0.1$ mJ/cm^2) for which the linear term dominates the decay dynamics, and provided an independent and consistent result for the unimolecular decay rate.

The Förster annihilation process is analogous to the well-known Förster resonance energy transfer process responsible for transfer of electronic excitation between molecules, $D^* + A \rightarrow D + A^*$. The energy transfer rate depends on the coupling of the donor and acceptor transition dipole moments, giving a rate varying as the inverse sixth power of the distance. Förster annihilation is typified by the process $S_1 + S_1 \rightarrow S_0 + S_n$, in which one exciton is de-excited while the other is promoted from the first excited state to a higher-lying electronic state. In this case, the relevant electronic transitions are $S_1 \rightarrow S_0$ emission and $S_1 \rightarrow S_n$ excited state absorption. Typically, fast intramolecular relaxation processes would be expected to return the excited molecule from the S_n state back to the S_1 state, so that the annihilation process results in the net loss of one of the two excitons. The strong $1/R^6$ distance dependence of the Förster process leads to a distribution of rates, as nearby excitons annihilate first, while remaining pairs of excitons at progressively larger distances give rise to progressively slower interaction rates. In the limit of spatially fixed excitations, the average of the distance-dependent rates over an ensemble of randomly distributed excitations gives rise to an effective $t^{-1/2}$ time-dependent annihilation rate [13]. While this treatment is in the limit of spatially fixed excitons, singlet exciton diffusion mediated by an $S_1 + S_0 \rightarrow S_0 + S_1$ Förster resonance energy transfer process can occur in molecular crystals. In C_{60}, it is likely that the long range annihilation rate dominates the exciton diffusion rate as a result of the strength of the $S_1 \rightarrow S_n$ electronic transition relative to the weak $S_0 \rightarrow S_1$ transition, consistent with the observation of the $t^{-1/2}$ behavior. We note that exciton annihilation following a $t^{-1/2}$ time dependence has been previously reported in thin films of phthalocyanine derivatives [15,16], with annihilation constants ranging from 1×10^{-16} to 6×10^{-15} cm^3 s$^{-1/2}$, similar in magnitude to that observed in C_{60}. Exciton annihilation rates with a $t^{-1/2}$ time dependence can also result from interaction of excitons within confined domains [17], though our comparison of the dynamics in thin film and crystalline samples, presented below, rules out this interpretation.

Additional insight into the dynamics can be gained by considering the limiting cases of high and low excitation densities. As discussed by Greene and Millard [15] for this regime of exciton annihilation, the initial decay of the excited state population at high excitation density is expected to be dominated by a single rate corresponding to annihilation of nearest-neighbor excitons. To investigate this limit for C_{60}, additional measurements were made at a laser fluence of 10 mJ/cm^2, corresponding to excitation of $\approx 25\%$ of the molecules in the fcc lattice. A linear fit to the initial slope of the natural logarithm of the decay trace gives a time constant of approximately 600 fs, indicating a rapid interaction between proximate excitons. At low excitation density, the relaxation dynamics in C_{60} are dominated by a unimolecular decay process with $1/\beta \approx 100$ ps. This value is of the same order as the singlet to triplet intersystem crossing rate observed for C_{60} in solution [18], indicating that this process may occur on a similar time scale in the solid.

The assignment of the nonexponential dynamics in solid C_{60} to exciton annihilation is further supported by measurements on crystalline samples. The primary difference between the crystalline samples and the thin film samples is the degree of long range order. Thin films grown under the conditions used for the samples in this study typically have lattice coherence lengths on the order of 10 nm, or just a few fcc unit cells [19], while X-ray diffraction peaks for crystalline samples are resolution limited, indicating a lattice coherence length > 150 nm. Fig. 2 shows traces of the time-resolved differential transmittance for crystalline C_{60}. The decay of the induced absorption is again nonexponential and strongly dependent on laser fluence. The observation of the same decay dynamics in crystalline and thin film samples rules out structural disorder as the origin of the nonexponential behavior. The apparent difference in the details of the response for the thin film samples in Fig. 1 and the crystalline samples in

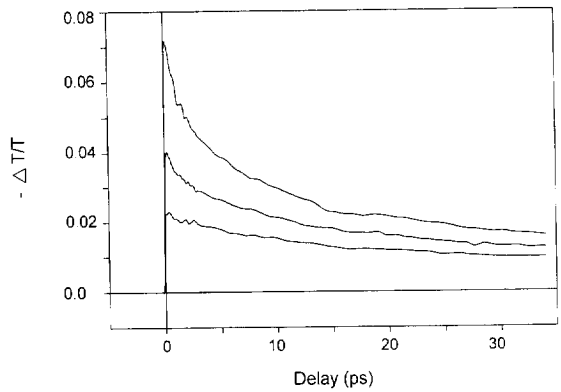

Fig. 2. Time-resolved negative differential transmittance of crystalline C_{60} under excitation conditions described in Fig. 1, with laser fluences (from top) of 1.3, 0.7, and 0.4 mJ/cm^2.

Fig. 2 can be attributed to the difference in optical density of the samples. In samples with a higher optical density, a wider range of excitation densities will be sampled throughout the depth of the sample in a transmission measurement, and since the decay dynamics depend strongly on excitation density, a slower decay curve representing the average over a range of excitation densities will result. We note that optical density effects may be responsible for some of the discrepancies among previously reported measurements of the nonexponential dynamics in C_{60}. To minimize this effect, the thin film measurements shown in Fig. 1, for which the sample optical density is only 0.14, were used for the quantitative determination of the rate constants. Comparison of the response observed for the crystals, which have an optical density of ≈ 0.6, with that from thin films of similar optical densities shows no significant difference in the decay dynamics for the two types of samples, consistent with the conclusion that interactions between localized molecular excitations, rather than the degree of disorder in the solid, are responsible for the nonexponential behavior. We also note that the stretched exponential function, which has been discussed in the context of dynamics in disordered systems, does not fit our thin film results over the full range of excitation densities covered in this study. As the excitation density is increased, fits to this function give unphysically small time constants, and at high excitation densities, the function no longer follows the time-resolved decay.

Finally, we note that for C_{60} in solution, where the molecules are well separated as a result of the limited solubility, no fast intensity-dependent dynamics are observed. Measurements extending to nanosecond time ranges have shown that the dynamics of C_{60} in solution are dominated by singlet to triplet intersystem crossing occurring on a time scale of several hundred picoseconds [18]. The absence of any fast intensity-dependent relaxation for C_{60} molecules isolated in solution is again consistent with the conclusion that in the solid, the fast relaxation results from interactions between photoexcitations rather than from intramolecular processes.

In conclusion, we have presented detailed measurements of the fast dynamics of solid C_{60} following photoexcitation, and have shown that the nonexponential response in the solid is consistent with a time-dependent exciton annihilation process. This conclusion is supported by the excellent fit between the data and the solution to the time-dependent rate equation over a range of excitation densities, as well as the comparison of the dynamics in thin film, crystalline, and solution phase samples. The absence of a significant dependence on probe wavelength is also consistent with excitonic interactions as the origin of the nonexponential dynamics. The exciton annihilation model reflects the molecular nature of solid C_{60} and provides a physically relevant mechanism for the nonexponential dynamics. The occurrence of exciton annihilation at high excitation densities is characteristic of other organic molecular crystals, although in C_{60}, the annihilation dynamics fall in an unusual motion-limited regime, giving rise to non-Markovian behavior.

This work was supported by the US Department of Energy under contract number DE-AC03-76SF00098. SLD acknowledges support from the University of California Office of the President and from the Los Alamos National Laboratory. The authors thank X.-D. Xiang for assistance with sample preparation.

References

[1] R.A. Cheville and N.J. Halas, Phys. Rev. B 45 (1992) 4548.
[2] M.J. Rosker, H.O. Marcy, T.Y. Chang, J.T. Khoury, K. Hansen and R.L. Whetten, Chem. Phys. Letters 196 (1992) 427.

[3] S.L. Dexheimer, D.M. Mittleman, R.W. Schoenlein, W. Vareka, X.-D. Xiang, A. Zettl, and C.V. Shank, in: Ultrafast phenomena, VIII, eds. J.L. Martin and A. Migus, (Springer, Berlin, 1992) p. 81; in: Ultrafast pulse generation and spectroscopy. eds. T.R. Gosnell, A.J. Taylor, K.A. Nelson and M.C. Downer, Proc. SPIE Vol. 1861 (SPIE, Bellingham, Washington, 1993) p. 328.

[4] S.D. Brorson, M.K. Kelly, U. Wenschuh, R. Buhleier and J. Kuhl, Phys. Rev. B 46 (1992) 7329.

[5] S.R. Flom, R.G.S. Pong, F.J. Bartoli and Z.H. Kafafi, Phys. Rev. B 46 (1992) 15598.

[6] T.N. Thomas, R.A. Taylor, J.F. Ryan, D. Mihailovic and R. Zamboni, in: Electronic properties of fullerenes, eds. H. Kuzmany, J. Fink, M. Mehring and S. Roth (Springer, Berlin, 1993) p. 292; Europhys. Letters 25 (1994) 403.

[7] S.B. Fleischer, E.P. Ippen, G. Dresselhaus, M.S. Dresselhaus, A.M. Rao, P. Zhou and P.C. Eklund, Appl. Phys. Letters 62 (1993) 3241.

[8] I.E. Kardash, V.S. Letokhov, Yu.E. Lozovik, Yu.A. Matveets, A.G. Stepanov and V.M. Farztdinov, JETP Letters 58 (1993) 138;
V.M. Farztdinov, Yu.E. Lozovik, Yu.A. Matveets, A.G. Stepanov and V.S. Letokhov, J. Phys. Chem. 98 (1994) 3290.

[9] T. Juhasz, X.H. Hu, C. Suarez, W.E. Bron, E. Maiken and P. Taborek, Phys. Rev. B 48 (1993) 4929.

[10] M.K. Kelly, P. Etchegoin, D. Fuchs, W. Krätschmer, and K. Fostiropoulos, Phys. Rev. B 46 (1992) 4963, and references therein.

[11] R.L. Fork, C.H. Brito Cruz, P.C. Becker and C.V. Shank, Opt. Letters 12 (1987) 483.

[12] K. Pichler, S. Graham, O.M. Gelsen, R.H. Friend, W.J. Romanow, J.P. McCauley Jr., N. Coustel, J.E. Fischer and A.B. Smith III, J. Phys. Condens. Matter 3 (1991) 9259.

[13] T. Förster, Z. Naturforsch. 4a (1949) 321.

[14] R.C. Powell and Z.G. Soos, J. Luminescence 11 (1975) 1.

[15] B.I. Greene and R.R. Millard, Phys. Rev. Letters 55 (1985) 1331.

[16] A. Terasaki, M. Hosoda, T. Wada, A. Yamada, H. Sasabe, A.F. Garito and T. Kobayashi, Mol. Cryst. Liq. Cryst. Sci. Technol. B 3 (1992) 161.

[17] G. Paillotin, C.E. Swenberg, J. Breton and N.E. Geacintov, Biophys. J. 25 (1979) 513.

[18] R.J. Sension, C.M. Philips, A.Z. Szarka, W.J. Romanov, A.R. McGhie, J.P. McCauley Jr., A.B. Smith III and R.M. Hochstrasser, J. Phys. Chem. 95 (1991) 6075.

[19] A.F. Hebard, R.C. Haddon, R.M. Fleming and A.R. Kortan, Appl. Phys. Letters 59 (1991) 2109.